

Variable Coordination Modes of Hydrotris(3-isopropyl-4-bromopyrazolyl)borate (Tp') in Fe(II), Mn(II), Cr(II), and Cr(III) Complexes: Formation of MTp'Cl (M = Fe and Mn), Structural Isomerism in CrTp'2, and the Observation of Tp'− as an Uncoordinated Anion

Tim J. Brunker, Tony Hascall, Andrew R. Cowley, Leigh H. Rees, and Dermot O'Hare*

Inorganic Chemistry Laboratory, South Parks Road, Oxford, U.K., OX1 3QR

Received January 30, 2001

The syntheses of the 4-coordinate Tp'MCl complexes (where M = Fe (**1**), Mn (**2**); and Tp' = hydrotris(3-isopropyl-4-bromopyrazolyl)borate) are described. The single-crystal X-ray structures show that the metal centers have distorted tetrahedral coordination. Analogous reaction of CrCl₂(MeCN)₂ with TITp' gave Cr(κ³-Tp')(κ²-Tp') (**3**) as the initial product. The 5-coordinate structure was assigned by single-crystal X-ray crystallography, and it was found that the κ³ ligand had isomerized to hydro(3-isopropyl-4-bromopyrazolyl)₂(5-isopropyl-4-bromopyrazolyl)borate). **3** is labile in solution: in pentane it slowly converts to the 6-coordinate isomer Cr(κ³-Tp')₂ (**4**), whose structure was determined by X-ray crystallography. In **4** both ligands are isomerized. Both **3** and **4** display Jahn–Teller distorted structures expected for high-spin d⁴ configurations. Variable temperature magnetic susceptibility measurements confirm that **1**, **2**, and **3** all have high-spin electronic configurations in the range 5–300 K. In benzene solution **3** decomposes; one product [Cr(κ³-Tp')₂]⁺[Tp'][−] (**5**), was identified by X-ray crystallography. **5** contains a pseudooctahedral Cr(III) cation with both ligands in the isomerized form and an uncoordinated Tp' ligand as counterion. Mechanistic studies reveal that this reaction is light rather than heat induced. IR spectroscopy is utilized to confirm the ligand hapticity in all complexes from the value of ν_{B–H}, and comparison is made with similar compounds.

Introduction

Tris(pyrazolyl)borate (Tp^{R,R'} = hydrotris(3-R-5-R'-pyrazolyl)borate)¹ ligands have proved very versatile reagents for the preparation of a huge range of metal sandwich and half-sandwich complexes, in part due to the large number of substitutable positions available on the pyrazole rings.^{2,3} Unsubstituted Tp and Tp^{Me2} have a great propensity to form MTp₂ complexes of high stability with first-row transition metal ions; however, bis coordination limits the further chemistry of such molecules.^{2,4,5} Incorporating a bulky substituent (e.g., *tert*-butyl) at the 3-position allows the selective formation of low-coordinate molecules, as this bulk prohibits the coordination of a second Tp ligand to the metal center. Such ligands are known as “tetrahedral enforcers” and have found wide utility as ancillary ligands for mimicking bioinorganic systems and in organometallic chemistry,^{3,6} where the steric protection of the metal has allowed the isolation of low-coordinate, electron-deficient compounds, unparalleled in the isoelectronic cyclopentadienyl chemistry.^{7–10} We have been interested in ligands that can stabilize such

4-coordinate (half-sandwich) type structures but are also able to expand their coordination to form full sandwich complexes. The previously reported Tp^{*i*-Pr,4-Br} (Tp') ligand shows such characteristics, stabilizing structures such as MTp'X (where M = Co, Ni, Zn and X = Cl, NCO, NCS),¹¹ MTp'L (where L = Tp and M = Fe, Co, Ni, Zn; L = Tp^{Me2}, Tp^{Ph} and M = Co, Ni) and MTp'₂ (M = Fe, Co, Ni).^{11,12} The MTp'₂ octahedral complexes are formed only by borotropic rearrangement of one pyrazolyl (pz) ring per ligand (i.e., to [HB(5-*i*-Pr-4-Brpz)(3-*i*-Pr-4-Brpz)₂][−]) which alleviates the severe steric strain a hypothetical unisomerized complex would possess. We were interested in exploring the half-sandwich chemistry of this ligand with earlier transition metals, and this paper reports the results of synthetic studies with Fe(II), Mn(II), and Cr(II) starting materials.

Experimental Section

All manipulations were carried under an inert atmosphere of dinitrogen using either standard Schlenk lines or in a Vac Atmospheres drybox unless otherwise stated. Solvents were distilled over potassium (THF), sodium–potassium alloy (pentane), sodium/benzophenone (diethyl ether), sodium (toluene), and calcium hydride (dichloromethane) under an atmosphere of dinitrogen. Infrared spectra were obtained as KBr disks. Ultraviolet/visible spectra were obtained as THF solutions in an airtight quartz cell. Elemental analyses were performed by the analytical department, Inorganic Chemistry Laboratory, Oxford. Mass spectra were obtained from the Mass Spectrometry Service, Dyson Perrins Laboratory, Oxford. Solid state magnetic susceptibility data were collected on a Quantum design MPMS-5 SQUID magnetometer. An

- (1) In the case where R = R', the abbreviation used is Tp^{R2}; e.g., hydrotris(3-methyl-5-methylpyrazolyl)borate is Tp^{Me2}.
- (2) Trofimenko, S. *Prog. Inorg. Chem.* **1986**, *34*, 115–209.
- (3) Trofimenko, S. *Chem. Rev.* **1993**, *93*, 943–980.
- (4) Trofimenko, S. *J. Am. Chem. Soc.* **1967**, *89*, 3170–3177.
- (5) Niedenzu, K.; Trofimenko, S. *Top. Curr. Chem.* **1986**, *131*, 1–137.
- (6) Kitajima, N.; Tolman, W. B. *Prog. Inorg. Chem.* **1995**, *43*, 419–531.
- (7) Jewson, J. D.; Liable-Sands, L. M.; Yap, G. P. A.; Rheingold, A. L.; Theopold, K. H. *Organometallics* **1999**, *18*, 300–305.
- (8) Kisko, J. L.; Hascall, T.; Parkin, G. *J. Am. Chem. Soc.* **1998**, *120*, 10561–10562.
- (9) Kersten, J. L.; Kucharczyk, R. R.; Yap, G. P. A.; Rheingold, A. L.; Theopold, K. H. *Chem. Eur. J.* **1997**, *3*, 1668–1674.
- (10) Akita, M.; Shirasawa, N.; Hikichi, S.; Moro-oka, Y. *Chem. Commun.* **1998**, 973–974.

- (11) Trofimenko, S.; Calabrese, J. C.; Domaille, P. J.; Thompson, J. S. *Inorg. Chem.* **1989**, *28*, 1091–1011.
- (12) Calabrese, J. C.; Domaille, P. J.; Thompson, J. S.; Trofimenko, S. *Inorg. Chem.* **1990**, *29*, 4429–4437.

accurately weighed powdered sample of ca. 50 mg was loaded, in a glovebox, into a gelatin capsule, which was packed in a drinking straw between additional gelatin capsules and lowered into the cryostat. Samples are therefore mounted in a weakly diamagnetic medium and no correction need be made for sample holder magnetism. Samples were checked for ferromagnetic impurities by measuring the magnetization vs field over a range of ± 5 T at 300 K. No impurities were revealed for **1**, **2**, or **3**; hence magnetic susceptibilities were measured using fields of 0.1 and 0.5 T, over the range 5–300 K. A correction for the inherent diamagnetism of the sample was estimated by use of Pascal's constants.¹³ $\text{FeCl}_2(\text{THF})_{3/2}$ was made by dehydration of commercial $\text{FeCl}_2 \cdot 4\text{H}_2\text{O}$ in vacuo (200 °C, 15 h), followed by stirring of the anhydrous solid in THF. The crude material obtained was then purified by continuous extraction with refluxing THF, cooling the resultant suspension to -30 °C, and isolation of the resultant solid. MnCl_2 was purchased from the Aldrich Chemical Co., CrCl_2 was purchased from Strem Chemicals Inc. KTp' ,¹¹ TITp' ,¹¹ and $\text{CrCl}_2(\text{MeCN})_2$ ¹⁴ were synthesized following the literature procedures.

Preparation of FeTp'Cl (1). To a stirred suspension of 0.29 g (1.22 mmol) of $\text{FeCl}_2(\text{THF})_{3/2}$ in 20 mL of THF was added, in one portion at room temperature, a solution of 0.75 g (1.22 mmol) KTp' in 15 mL of THF. The reaction mixture was stirred for 12 h and then filtered through a bed of Celite on a glass sintered frit, to give a clear golden solution. All volatiles were removed in vacuo and the residue was extracted with hot toluene; cooling the extracts to -30 °C yielded analytically pure solid as a white powder. Single crystals were grown by layering 10 mL of a saturated CH_2Cl_2 solution of the compound with 50 mL of pentane. Yield: 0.34 g (45.5%).

Anal. Calcd: C, 32.40; H, 3.78; N, 12.59. Found: C, 33.10; H, 3.81; N, 12.49; IR (KBr disk) ν (cm^{-1}): 2971(s), 2931(m), 2871(w), 2504(m), 1510(m), 1484(m), 1460(w), 1369(s), 1297(m), 1142(s), 1083(s), 1040(s), 832(m), 744(m), 657(w). MS (EI): m/z 667.81 (M^+ , 100%), 630.83 ($\text{M}^+ - \text{Cl}$, 20%), 522.78 ($\text{M}^+ - \text{Cl} - \text{Br} - 2\text{Me}$, 30%), 478.33 ($\text{M}^+ - \text{Cl} - \text{Br} - 2\text{Me} - i\text{-Pr}$, 32%), 441.86 ($\text{M}^+ - \text{Cl} - \text{pz}'\text{H} - \text{H}$, 20%). ^1H NMR (300 MHz, CD_3CN): δ 27.0 (s, br), 7.5 (s, br), -28.7 (s, br). Magnetic moment (SQUID): $5.36 \mu_{\text{B}}$ (300 K).

Preparation of MnTp'Cl (2). To a stirred suspension of 0.21 g (1.63 mmol) of MnCl_2 in 20 mL of THF was added, in one portion at room temperature, a solution of 1.00 g (1.63 mmol) of KTp' in 20 mL of THF. The reaction mixture was stirred for 12 h and then filtered through a bed of Celite on a glass sintered frit, to give a clear pale golden solution. All volatiles were removed in vacuo and the residue was extracted with hot toluene; cooling the extracts to -30 °C yielded analytically pure solid as a white powder. Crystals suitable for single-crystal X-ray diffraction were grown by slow cooling of a concentrated dichloromethane solution to -30 °C. Yield: 0.58 g (52.9%).

Anal. Calcd: C, 32.45; H, 3.78; N, 12.61; Mn, 8.24. Found: C, 33.09; H, 3.81; N, 12.49; Mn, 8.22. IR (KBr disk) ν (cm^{-1}): 2968(s), 2928(m), 2868(w), 2506(m), 1506(m), 1486(m), 1458(w), 1364(s), 1292(m), 1136(s), 1084(s), 1038(s), 832(m), 744(m), 654(w). MS (EI): m/z 666.92 (M^+ , 5%), 629.06 ($\text{M}^+ - \text{Cl} - \text{H}$, 100%), 551.14 ($\text{M}^+ - \text{Cl} - \text{Br}$, 7%), 521.95 ($\text{M}^+ - \text{Cl} - \text{Br} - 2\text{Me}$, 9%), 477.96 ($\text{M}^+ - \text{Cl} - \text{Br} - 2\text{Me} - i\text{-Pr}$, 18%). Magnetic moment (SQUID): $5.85 \mu_{\text{B}}$ (300 K).

Preparation of Two Isomers of CrTp'2, (3) and (4). To a stirred suspension of $\text{CrCl}_2(\text{MeCN})_2$ (0.192 g, 1.01 mmol) in 10 mL of toluene was added a solution of TITp' (0.729 g, 1.01 mmol) in toluene (20 mL) with stirring. The reaction mixture was stirred for 5 h, during which time large amounts of white solid were seen to precipitate. The reaction mixture was filtered through Celite to give a clear purple solution; all volatiles were then removed in vacuo. The resultant light purple solid was extracted with warm pentane (3×15 mL) and cooled to -30 °C for 24 h. The resultant purple powder was isolated by filtration. Single crystals of **3** were grown by redissolving this solid in pentane (20 mL) and slow cooling the solution to -30 °C for 3 days. The filtrate from above was reduced in volume and again cooled to -30 °C. A mixture of blue and purple crystalline solid was isolated

after 36 h. After several days standing the pentane filtrate yielded crystals of **4** suitable for single-crystal X-ray diffraction. Total yield of both **3** and **4**: 0.380 g (62% based on TITp').

Anal. Calcd for $\text{CrC}_{36}\text{H}_{50}\text{N}_{12}\text{Br}_6\text{B}_2\text{C}_5\text{H}_{12}$: C, 38.59; H, 4.90; N, 13.17; Found: C, 38.06; H, 4.82; N, 13.27. IR (KBr disk) ν (cm^{-1}): **3**: 3135(m), 2969(vs), 2933(s), 2872(s), 2494(m), 2369(m), 1511(s), 1480(s), 1456(s), 1369(br, vs), 1287(s), 1240(s), 1218(s), 1171(br,vs), 1137(br,vs), 1050(vs), 1007(s), 983(s), 973(s), 928(w), 884(m), 835(m), 799(m), 742(s), 726(s), 654(s), 450(w), 419(m); **4**: 3129(m), 2966(s), 2932(s), 2872(s), 2524(m), 2489(m), 1636(w), 1511(s), 1480(s), 1457(s), 1365(vs), 1310(s), 1288(s), 1227(s), 1184(vs), 1166(vs), 1138(vs), 1045(vs), 1026(s), 992(s), 884(m), 864(m), 833(m), 823(m), 798(m), 743(s), 723(s), 665(m), 650(m), 438(w), 416(w). MS (EI): m/z 1203.7 (M^+ , 100%). Magnetic moment (SQUID), **3**: $5.05 \mu_{\text{B}}$ (300 K). UV/vis **3**: λ_{max} 535 nm (ϵ 40 $\text{M}^{-1} \text{cm}^{-1}$), 305 nm (ϵ 1400 $\text{M}^{-1} \text{cm}^{-1}$).

5 was isolated as pink-orange air-stable crystals from a solution of **3** (~ 10 mg) in dry d^6 -benzene (1 mL) (sealed in an NMR tube fitted with a Young's type concentric stopcock under N_2) that had been standing under laboratory lights for 4 weeks. The same product (according to IR spectroscopy) was isolated as pink-orange microcrystals from a solution of **3** (50 mg) in dry C_6H_6 (6 mL) left to stand under N_2 for the same length of time. Solutions of **3** of the same concentration heated in an evacuated ampule in the dark for 10 days showed no color change or deposited any solids; however, the same solution on photolysis for 2 h with a Hanovia, 500 W UV lamp turned a pale/green yellow color. Removal of all volatiles in vacuo and extraction with pentane left a small amount of a pale green solid whose IR was similar to that obtained with the previous samples.

IR (KBr disk) ν (cm^{-1}): 3121(m), 2967(s), 2932(s), 2870(m), 2529(w), 2460(w), 2364(w), 2342(w), 1637(m), 1510(m), 1480(m), 1459(m), 1378(s), 1363(s), 1319(w), 1288(w), 1230(m), 1182(s), 1164(s), 1138(vs), 1055(s), 1044(s), 1025(m), 998(m), 803(m), 739(m), 720(m), 680(s), 654(m), 578(w), 463(w), 437(w).

Crystal Structure Determination. The X-ray data for all compounds were collected at 150 K using graphite-monochromated $\text{Mo K}\alpha$ ($\lambda = 0.71073$ Å) radiation using an Enraf-Nonius DIP2000 image plate diffractometer. Intensity data were processed using the programs DENZO and SCALEPACK.¹⁵ The structures were solved using the direct-methods program SIR-92¹⁶ in space groups $Ccm2_1$ (**1**, **2**) and $P\bar{1}$ (**3**–**5**), and subsequent full-matrix least-squares refinement was carried out on all F^2 using SHELX-93¹⁷ (**1**–**4**) and on F using the CRYSTALS¹⁸ program suite (**5**). Crystallographic data are summarized in Table 1. For **1**–**4** all non-hydrogen atoms were refined anisotropically and hydrogen atoms were included in calculated positions with isotropic thermal parameters. In **3**, the asymmetric unit was also found to contain a molecule of pentane. Residual electron density in the asymmetric unit of **4** was also attributed to half a molecule of pentane of crystallization. This was modeled as a composite of two half-occupied orientations related to one another by a one-atom displacement along the alkane chain. For **5** the coordinates and anisotropic thermal parameters of all non-hydrogen atoms were refined. Hydrogen atoms were positioned geometrically after each cycle of refinement. Refinement converged to give unsatisfactory residual electron densities (-2.7 , $+5.2$ e \AA^{-3}). Careful examination of a difference Fourier map showed one of the pyrazolyl groups of the free Tp' anion to be disordered, with ca. 90% of the sites occupied by a pyrazolyl ring linked to boron through N2 and the remainder linked through N1. An acceptable model of the disorder was constructed in which the two bromine atoms were

(13) O'Conner, C. J. *Prog. Inorg. Chem.* **1982**, *29*, 203–283.

(14) Holah, D. G.; Fulder, J. P. *Inorg. Synth.* **1967**, *10*, 31.

(15) Otinowski, Z.; Minor, W. *Processing of X-ray Diffraction Data Collected in Oscillation Mode*; Methods in Enzymology 276; Carter C. W., Sweet, R. M., Eds.; Academic Press: New York, 1997; pp 307–326.

(16) Altomare, A.; Cascarano, G.; Giacovazzo, G.; Guagliardi, A.; Burla, M. C.; Polidori, G.; Camalli, M. *J. Appl. Crystallogr.* **1994**, *27*, 343–350.

(17) Sheldrick, G. M. *SHELX-93—Program for Crystal Structure Refinement*; Institut für Anorganische Chemie der Universität, Tammanstrasse 4, D-3400, Göttingen, Germany, 1993.

(18) Watkin, D. J.; Prout, C. K.; Carruthers, J. R.; Betteridge, P. W. *CRYSTALS* issue 10; Chemical Crystallography Laboratory, Oxford, UK, 1996.

Table 1. Crystallographic Data for **1**–**5**

	1	2	3	4	5
formula	C ₁₈ H ₂₅ BBR ₃ ClFeN ₆	C ₁₈ H ₂₅ BBR ₃ ClMnN ₆	C ₄₁ H ₆₂ B ₂ Br ₆ CN ₁₂ [3·C ₅ H ₁₂]	C _{38.5} H ₅₆ B ₂ Br ₆ CrN ₁₂ [4·(C ₅ H ₁₂) _{0.5}]	C ₇₂ H ₉₃ B ₃ Br ₉ CN ₁₈ [5·(C ₆ H ₆) ₃]
fw	667.28	666.37	1276.11	1240.03	2014.2
cryst syst	orthorhombic	orthorhombic	triclinic	triclinic	triclinic
space group	<i>Ccm</i> 2 ₁	<i>Ccm</i> 2 ₁	<i>P</i> $\bar{1}$	<i>P</i> $\bar{1}$	<i>P</i> $\bar{1}$
<i>a</i> , Å	10.870(1)	10.781(1)	10.126(1)	12.982(1)	12.576(1)
<i>b</i> , Å	14.462(1)	14.314(1)	14.329(1)	13.065(1)	12.760(1)
<i>c</i> , Å	15.798(1)	15.768(1)	20.877(2)	15.927(1)	29.964(1)
α , deg	90	90	107.851(5)	98.032(4)	86.300(3)
β , deg	90	90	91.252(4)	105.392(3)	81.231(3)
γ , deg	90	90	109.921(4)	101.759(3)	62.911(2)
<i>V</i> , Å ³	2483.5	2433.3(1)	2683.7(3)	2495.5(3)	4230.7
<i>Z</i>	4	4	2	2	2
<i>D</i> (calcd), Mg m ⁻³	1.79	1.82	1.58	1.65	1.58
μ , mm ⁻¹	5.56	5.60	4.72	5.07	4.44
<i>F</i> (000)	1312	1308	1272	1230	2004
GOF	1.018	1.044	1.000	1.006	1.110
final <i>R</i> indices	R1 = 0.0291, wR2 = 0.0661 ^a	R1 = 0.0199, wR2 = 0.0484 ^a	R1 = 0.0599, wR2 = 0.1320 ^a	R1 = 0.0417, wR2 = 0.1007 ^a	R1 = 0.0540, wR2 = 0.0426 ^b
residuals ρ (e Å ⁻³)	0.41, -0.39	0.65, -0.40	1.77, -1.81	0.98, -0.87	0.97, -0.89

^a For [*I* > 2 σ]. ^b For [*I* > 3 σ].

refined anisotropically, as was the more highly occupied isopropyl substituent, while the less highly occupied isopropyl group was modeled isotropically. The overlapping atoms of the pyrazole rings were modeled with common coordinates and anisotropic thermal parameters. Occupancies of the two sites were refined, subject to the constraint that their sum was unity. Refinement converged satisfactorily, and the small values of the residual electron densities indicated that the model of the disorder was appropriate; however, distinct positions could not be resolved for the two pyrazole rings and thus the geometric parameters of these groups have little meaning.

Results and Discussion

It was found that a simple metathesis reaction between KTp' and a convenient anhydrous MCl₂ source utilizing THF as solvent was a suitable method for synthesizing the Mn and Fe half-sandwich complexes MTp'Cl (M = Fe (**1**), Mn (**2**)). Both **1** and **2** are air-stable, colorless solids although **1** slowly decomposes even when stored in a glovebox. They are soluble in toluene and polar solvents such as CH₂Cl₂ and MeCN. The monomeric nature of the structures was confirmed by single-crystal X-ray diffraction. ¹H NMR spectroscopy displayed broadened, overlapping peaks and was not a useful tool for characterizing these compounds; however, IR spectroscopy provided a distinctive fingerprint pattern. Magnetic measurements are consistent with the formulation of **1** and **2** as high-spin d⁶ and d⁵ metal centers, respectively (Figure 2). **1** obeys the Curie–Weiss law with a moment of 5.36 μ_B at 300 K (values of *C* = 3.63 emu K/mol, θ = 1.11 K by fitting data to the Curie–Weiss law over the range 50–300 K) which drops to ~4.8 μ_B at 5 K: a room temperature moment greater than the spin-only value is consistent with the large second-order spin–orbit coupling contribution expected for a pseudotetrahedral d⁶ ion. The moment of **2** agrees well with the spin-only value for a d⁵ ion (μ_{eff} = 5.85 μ_B at 300 K, *C* = 4.28 emu K/mol, θ = -0.09 K fitted over the range 5–300 K) and varies little with temperature.

1 and **2** are both isostructural with the previously reported CoTp'Cl,¹⁹ and a view of **2** is shown in Figure 1. Lists of important bond lengths and angles are given in Table 2. Both Fe and Mn centers lie in a trigonally distorted tetrahedral environment with N–M–N and N–M–Cl bond angles in the

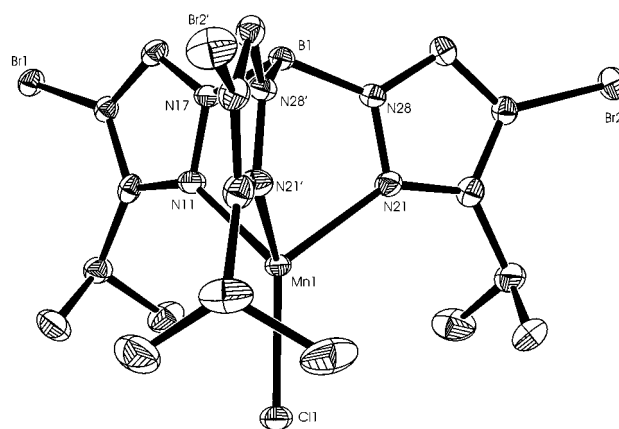


Figure 1. Molecular structure of **2** with thermal ellipsoids at 50% probability, showing the atom labeling scheme; primed atoms are symmetry generated (hydrogen atoms are omitted for clarity). **1** and **2** have identical numbering schemes.

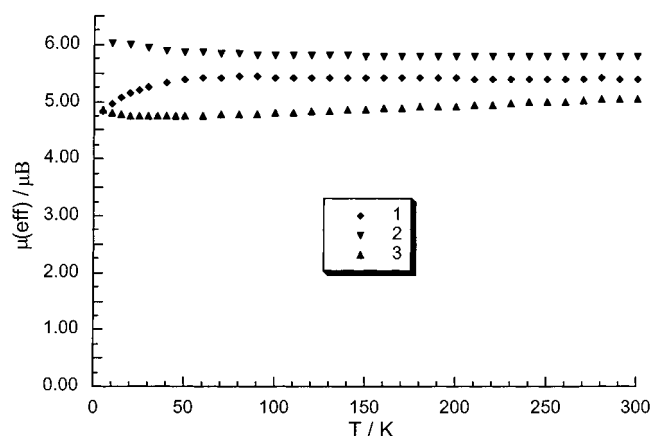


Figure 2. Plot of μ_{eff} (μ_B) against temperature (K) for **1** (◆), **2** (▼), and **3** (▲).

ranges 91.4°–92.0° and 124.0°–124.4° for **1**, and 90.0°–90.9° and 125.0°–125.2° for **2**. The Fe–Cl bond length in **1** (2.224(2) Å) is essentially the same as those in the previously reported FeTpⁱ-BuCl²⁰ (2.227(2) Å) and Tpⁱ-Pr²FeCl²¹ (2.204(2) Å). The

(19) Olson, M. D.; Rettig, S. J.; Storr, A.; Trotter, J.; Trofimenko, S. *Acta Crystallogr., Sect. C* **1991**, *C47*, 1543–1544.

(20) Gorrell, I. B.; Parkin, G. *Inorg. Chem.* **1990**, *29*, 2452–2456.

Table 2. Selected Bond Lengths and Angles in **1** and **2**

1		2	
Fe1–N11	2.099(5)	Mn1–N11	2.128(5)
Fe1–N21	2.084(4)	Mn1–N21	2.132(3)
Fe1–Cl1	2.224(2)	Mn1–Cl1	2.272(2)
B1–N17	1.548(8)	B1–N17	1.550(6)
B1–N28	1.546(8)	B1–N28	1.539(4)
N11–Fe1–N21	91.48(13)	N11–Mn1–N21	90.02(11)
N21'–Fe1–N21	92.00(2)	N21'–Mn1–N21	90.9(2)
N11–Fe1–Cl1	124.37(14)	N11–Mn1–Cl1	125.16(13)
N21–Fe1–Cl1	123.96(10)	N21–Mn1–Cl1	124.99(8)

Fe–N bond lengths in **1** (2.099(5) and 2.088(4) Å) display a slight lengthening relative to FeTp^{i-Pr}2Cl (2.054(5) and 2.053(4) Å): this reflects the tightening of the “bite” of the ligand with isopropyl groups in the 5-positions and has been attributed to nonbonding repulsions between these groups.³ The Mn–Cl bond length 2.272(2) Å is significantly shorter than that in another reported Mn(II) complex with pyrazole ligands—[MnCl{H₂B(pz)₂}₂][AsPh₄]⁺ (2.373(2) Å)²² and slightly shorter than that in the tetrahedral complex MnCl₂(Ph₃PO)₂ (2.294(3) Å).²³

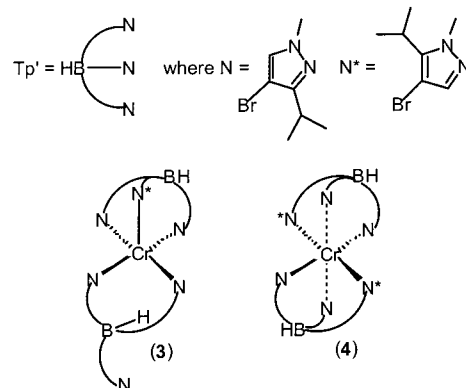
Under the same conditions used to synthesize **1** and **2**, reaction with anhydrous CrCl₂ proved less reproducible, and it was difficult to isolate any crystalline products. Mass spectral analysis of the resultant blue powders from such reactions indicated the presence of species such as CrTp'Cl and CrTp'Cl-(pzH). Similar observations have been made in the reaction of CrCl₂ with KTp^{i-Bu,Me} where the compound CrTp^{i-Bu,Me}Cl(3-*t*-Bu-5-MepzH) was isolated and crystallographically characterized and shows a free pyrazole ring bound to the metal through a single N atom.⁹ ¹H NMR spectroscopy of crude KTp' in *d*⁵-pyridine reveals the presence of varying amounts of residual pyrazole. The low solubility of KTp' even in polar solvents precluded all attempts to purify this salt by recrystallization, so in order to eliminate this complication, we decided to utilize TITp' which can be easily purified by recrystallization from toluene, in which it is reasonably soluble. The solvated Cr(II) starting material CrCl₂(MeCN)₂ reacted cleanly and reproducibly with 1 or 2 equiv of TITp' in toluene to form purple material **3**, which was recrystallized from pentane, in which it is reasonably soluble (decomposition was seen to occur in CH₂Cl₂ solution). It was found that, as well as containing **3**, a subsequent crop of crystals contained also blue crystalline material, the supernatant from which produced, on standing, solely bright blue crystals of **4**. The IR spectra of **3** and **4** were essentially the same apart from significant differences in the B–H region: **3** displayed two sharp bands at 2496 and 2368 cm⁻¹, whereas **4** displayed overlapping bands at 2524 and 2489 cm⁻¹. This suggested that neither compound was the expected CrTp'Cl. Single-crystal X-ray diffraction showed both products to be isomers of CrTp'₂. **3** and **4** are 5- and 6-coordinate, respectively. These products were observed when either 1 or 2 equiv of TITp' were used and no CrTp'Cl products were observed under these conditions.

The Tp' ligand has been observed to form bis(Tp) octahedral complexes; however, this only occurred with rearrangement of the ligand to HB[(3-*i*-Pr-4-Br-pyrazolyl)₂(5-*i*-Pr-4-Br-pyrazolyl)] via a 1,2-borotropic rearrangement of one pyrazole ring per ligand.¹¹ The Tp^{i-Pr} ligand exhibits the same behavior—in both cases this has been attributed to the inability of the molecule to accommodate six isopropyl groups in the equatorial positions.³

(21) Ito, M.; Amagai, H.; Fukui, H.; Kitajima, N.; Moro-oka, Y. *Bull. Chem. Soc. Jpn.* **1996**, *69*, 1937–1945.

(22) Di Vaira, M.; Mani, F. *J. Chem. Soc., Dalton Trans.* **1990**, 191–194.

(23) Tomita, K. *Acta Crystallogr., Sect. C* **1985**, *C41*, 1832–1833.

**Figure 3.** Schematic representation of the Tp' ligand coordination in **3** and **4**.

3 provides an intermediate case in which one of the Tp' ligands has isomerized and is coordinated in a κ^3 fashion, while the second binds in a κ^2 manner and remains unisomerized, making the Cr center 5-coordinate. In **4** both ligands have isomerized and bind in a κ^3 , albeit highly distorted, fashion to the Cr center: the isomerization of the second ligand seems to occur slowly in solution and suggests that the 6-coordinate structure is actually the more energetically favorable. A schematic of the Cr coordination sphere in **3** and **4** is given in Figure 3. In **3** the Cr center is surrounded by five N atoms in a pyramidal arrangement, the axial position being occupied by N21 which belongs to the isomerized pyrazole ring. The axial Cr–N21 bond length (2.278(6) Å) is significantly longer than the Cr–N bond lengths in the equatorial belt, which vary in the range 2.099(5)–2.127(5) Å. The B–H bond of the κ^2 ligand points toward the vacant octahedral site; however, the Cr–H2 distance of 2.789 Å is considerably longer than a crystallographically determined agostic Cr···H–C interaction (2.240 Å),²⁴ and any interaction present is undoubtedly very weak. Nevertheless, some weakening of this B–H bond is indicated by IR data: ν_{B-H} assigned to the κ^2 ligand lies at 128 cm⁻¹ lower than that assigned to the κ^3 ligand. A detailed analysis of the variation of ν_{B-H} with hapticity in MTP^{i-Pr}2L_n complexes concluded that ν_{B-H} is indicative of coordination mode and for κ^2 ligands lies at frequencies 40–50 cm⁻¹ lower than those for the corresponding κ^3 ligand.²⁵ A Co complex of similar geometry [Co(κ^3 -Tp^{Ph})(κ^2 -Tp^{Ph})] displays a much stronger agostic Co···H–B interaction with a Co–H distance of 2.17 Å, and the B–H bands are reported at 2467 and 2176 cm⁻¹, the lowering by 291 cm⁻¹ of the κ^2 ligand stretch indicating the greater strength of this interaction in this complex.²⁶ CoTp'L compounds with agostic Co–H–B bonds have been reported (where L = Tp^{Ph} and is sterically prevented from binding κ^3 , and L = H₂B(pz)₂), but not in the case where L = Tp'.¹²

A comparison of the N–Cr–N bond angles in the coordination sphere (see Table 4) with regular square-pyramidal and octahedral geometry²⁷ reveals an average deviation of 9.6° from square pyramidal. If we assume the geometry to be octahedral but with a missing apex, then the deviation is only 6.3° (if H2 is assumed to be part of the coordination sphere, then the average deviation is 9.6°). The N–B–N bond angles reflect the

(24) Zhang, K.; Gonzalez, A. A.; Mukerjee, S. L.; Chou, S.-J.; Hoff, C. D.; Kubat-Martin, A.; Barnhart, D.; Kubas, G. J. *J. Am. Chem. Soc.* **1991**, *113*, 9170–9176.

(25) Akita, M.; Ohta, K.; Takahashi, Y.; Hikichi, S.; Mora-Oka, Y. *Organometallics* **1997**, *16*, 4121–4128.

(26) Kremer-Aach, A.; Klau, W.; Bell, R.; Strerath, A.; Wunderlich, H.; Mootz, D. *Inorg. Chem.* **1997**, *36*, 1552–1563.

(27) Zeeman, J. Z. *Anorg. Allg. Chem.* **1963**, *324*, 241.

Table 3. Selected Bond Lengths and Angles in **3** and **4**

3		4	
Cr–N31	2.099(5)	Cr–N21	2.066(3)
Cr–N41	2.107(5)	Cr–N51	2.074(3)
Cr–N11	2.111(5)	Cr–N11	2.145(3)
Cr–N51	2.127(5)	Cr–N41	2.176(3)
Cr–N21	2.278(6)	Cr–N31	2.421(3)
N12–B1	1.545(10)	Cr–N61	2.520(3)
N22–B1	1.540(10)	N12–B1	1.536(6)
N32–B1	1.553(9)	N22–B1	1.546(6)
N42–B2	1.556(9)	N32–B1	1.537(7)
N52–B2	1.545(10)	N42–B2	1.555(5)
N62–B2	1.504(10)	N52–B2	1.545(6)
N31–Cr–N41	172.4(2)	N62–B2	1.539(6)
N31–Cr–N11	83.2(2)	N21–Cr–N51	177.13(14)
N41–Cr–N11	90.6(2)	N21–Cr–N11	84.15(13)
N31–Cr–N51	97.7(2)	N51–Cr–N11	93.01(13)
N41–Cr–N51	87.6(2)	N21–Cr–N41	94.10(13)
N11–Cr–N51	168.2(2)	N51–Cr–N41	88.63(13)
N31–Cr–N21	85.1(2)	N11–Cr–N41	169.52(12)
N41–Cr–N21	99.4(2)	N21–Cr–N31	89.73(13)
N11–Cr–N21	92.1(2)	N51–Cr–N31	89.58(12)
N51–Cr–N21	99.7(2)	N11–Cr–N31	83.39(13)
N22–B1–N12	110.9(6)	N41–Cr–N31	86.27(12)
N22–B1–N32	110.0(6)	N21–Cr–N61	99.55(12)
N12–B1–N32	106.6(6)	N51–Cr–N61	81.71(12)
N62–B2–N52	112.1(6)	N11–Cr–N61	109.23(12)
N62–B2–N42	110.3(6)	N41–Cr–N61	81.25(11)
N52–B2–N42	106.6(6)	N31–Cr–N61	164.91(12)

Table 4. Deviation of the Observed Angles (deg) in **3** from Regular Square Pyramidal (SQP) and Octahedral (O) Geometry

angle	obsd	SQP	Δ (SQP)	O	Δ (O)
N21–Cr–N11	92.0	104.1	12.1	90.0	2.0
N21–Cr–N31	85.1	104.1	19.0	90.0	4.9
N21–Cr–N41	99.5	104.1	4.6	90.0	9.5
N21–Cr–N51	99.7	104.1	4.4	90.0	9.7
N11–Cr–N31	83.3	86.6	3.3	90.0	6.7
N11–Cr–N41	90.5	86.6	3.9	90.0	0.5
N31–Cr–N51	97.7	86.6	11.1	90.0	7.7
N51–Cr–N41	87.6	86.6	1.0	90.0	2.4
N11–Cr–N51	168.3	151.9	16.4	180.0	11.7
N31–Cr–N41	172.4	151.9	20.5	180.0	7.6
H2–Cr–N21	164.8			180.0	15.2
H2–Cr–N31	105.3			90	15.3
H2–Cr–N41	71.5			90	19.5
H2–Cr–N51	68.4			90	21.6
H2–Cr–N11	100.1			90	10.1

associated distortion of the B centers away from perfect tetrahedral geometry: in the κ^3 ligand there is a tightening of the angle between the equatorial rings (N12–B1–N32, 106.6°) as compared to the angles between the axially and equatorially coordinated rings (110.2° and 110.9°). Similarly in the κ^2 ligand, the angle between the two bound rings (N42–B2–N52, 106.7°) is significantly tighter than the unbound-ring–B–bound-ring angles (110.3° and 112.3°).

4 can be described as a 6-coordinate structure, but a large distortion away from regular octahedral geometry results in Cr–N distances of 2.421 (N31) and 2.520 Å (N61) to the axial positions. In contrast, the equatorial bond lengths fall into two groups: the shorter bonds (Cr–N21 2.066(3) Å and Cr–N51 2.074(3) Å) are to the rings with the isopropyl group in the 5-position and lie trans to one another, while the longer bonds (Cr–N11 2.145(3) Å and Cr–N41 2.176(3) Å) lie on the perpendicular axis and are to unisomerized pyrazoles. The axial N atoms are not truly coaxial with Cr as evidenced by the N31–Cr–N61 angle of 164.9°, and there is subsequently significant deviation of N61–Cr–N_{eq} and N31–Cr–N_{eq} bond angles from 90° (81.3°–109.2° and 83.4°–89.7° respectively). Similar irregularity is seen in the N–Cr–N angles between substituents

in the equatorial positions with angles varying between 84.2° and 94.1°, the tighter angles being between rings of the same ligand.

To our knowledge there is no other example of a bis(Tp) Cr(II) complex that has been structurally characterized: Mani et al. report the syntheses of CrTp₂, Cr[B(pz)₄]₂ and Cr[H₂B(pz)₂]₂, although only the structure of the latter was determined.²⁸ Cotton et al. also report the X-ray structure of Cr[Et₂B(pz)₂]₂.²⁹ In both cases the 4-coordinate Cr site displays regular square-planar geometry with only very minor differences in N–Cr–N bond angles and in Cr–N bond lengths (2.055(4), 2.066 and 2.058(4), 2.061(4) Å, respectively), which are very similar to the short bonds in **4**. Other crystallographically characterized Cr(II) compounds with Tp ligands are those based on the tetrahedral-enforcer ligand Tp^{–Bu,Me}:⁹ the 4-coordinate compounds CrTp^{–Bu,Me}(X) (where X = Cl, Et, Ph) instead of adopting a typical C_{3v} MTPX structure, such as displayed by **1** and **2**, adopt a structure which can be regarded as a cis-divacant octahedral structure or as a pseudotetrahedral structure in which the X ligand is displaced off the 3-fold axis. This unusual geometry is a manifestation of a Jahn–Teller distortion expected for a high-spin d⁴ tetrahedral complex. The gross deviations from regular octahedral geometry displayed by **3** and **4** are also readily explained as Jahn–Teller effects. There is a depletion of electron density available for bonding along the elongated axis with two long Cr–N bonds in **4** or a single slightly shorter bond in **3** providing sufficient bonding. The comparative regularity of the coordinated geometry of the isomerized ligands in **5** (vide infra) indicates that steric crowding is not the origin of these distortions. It is interesting to note that the isomerized pyrazole ring takes up an axial position in **3**, while in **4** they both bind to an equatorial site. The exact conformations of **3** and **4** must depend on a subtle interplay of steric and electronic effects: the isolation of both structure types probably indicates that there is only a small stabilization associated with isomerization of the second Tp' ligand, and with formation of a sixth, weak Cr–N bond. Magnetic measurements confirm that **3** has a high-spin d⁴ configuration: $\mu_{\text{eff}} = 5.05 \mu_{\text{B}}$ at 300 K is close to the expected spin-only value for $S = 2$, and the moment shows Curie–Weiss behavior over the full temperature range ($C = 3.17 \text{ emu K/mol}$, $\theta = -6.49 \text{ K}$). Insufficient sample was available to perform measurements on **4**.

The lability of the Tp' ligand is further illustrated by the isolation of **5**. It was found that solutions of **3** in dry C₆D₆ or C₆H₆, after standing under laboratory lights for periods of weeks, deposited air-stable orange-pink crystals. A single-crystal X-ray study indicated this product to be [CrTp'₂]⁺[Tp][–]·3C₆D₆, the Cr(III) analogue of **4** with a noncoordinated Tp' anion as the counterion. This so-called “ κ^0 ” mode is most unusual, but not unprecedented: Carmona et al. have recently reported the crystal structure of [Rh(H)₂(PMe₃)₄]⁺[Tp][–], synthesized from [Rh(H)₂(PMe₃)₂Tp] by addition of excess PMe₃.³⁰ In our structure the Tp' anion shows disorder in one of the pyrazole rings corresponding to the presence of both structural isomers with the isopropyl group in the 3- or 5-position (in ratio 0.819(2):0.181(2)). These are positioned in such a way that the atoms of the five-membered ring overlap as shown in Figure 7. The geometry around B is essentially tetrahedral (N72–B3–N82 bond angle of 108.9°) with B–N bond lengths similar to those in the coordinated ligand (N72–B3 1.526(7) Å and N82–B3 1.560-

(28) Dapporto, P.; Mani, F.; Mealli, C. *Inorg. Chem.* **1978**, *17*, 1323–1329.

(29) Cotton, F. A.; Mott, G. N. *Inorg. Chem.* **1983**, *22*, 1136–1139.

(30) Paneque, P.; Sirol, S.; Trujillo, M.; Gutierrez-Puebla, M.; Angeles Monge, M.; Carmona, E. *Angew. Chem., Int. Ed.* **2000**, *39*, 218–221.

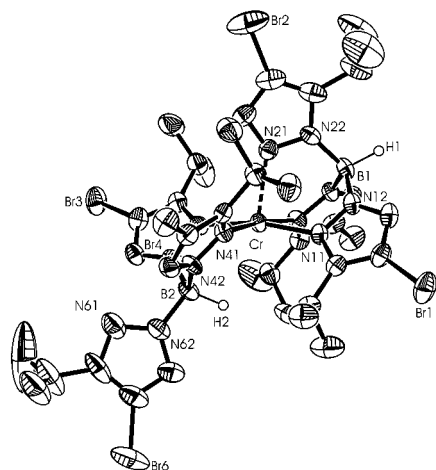


Figure 4. Molecular structure of **3** with thermal ellipsoids at 50% probability (hydrogen atoms are omitted for clarity).

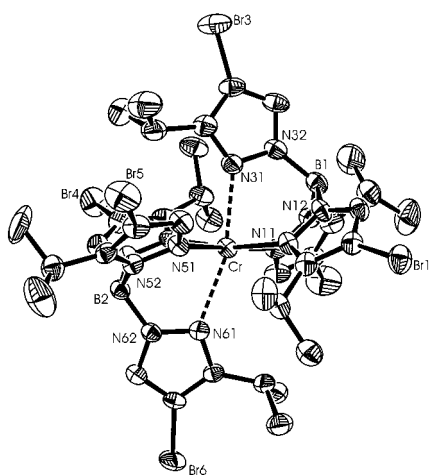


Figure 5. Molecular structure of **4** with thermal ellipsoids at 50% probability (hydrogen atoms are omitted for clarity).

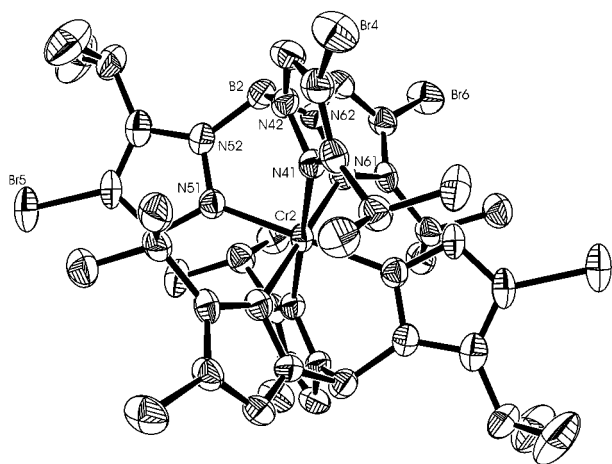


Figure 6. Molecular structure of one of the crystallographically independent $[\text{Tp}'_2\text{Cr}]$ cations in **5** (Cr lies on an inversion center), showing the labeling scheme, with thermal ellipsoids at 50% probability (hydrogen atoms are omitted for clarity).

(7) Å, as opposed to 1.509(7)–1.547(6) Å). The orientation of the pyrazoles in almost orthogonal planes as shown in Figure 8 and the lack of any short contact distances from the N atoms confirm that this is indeed a free anion.

In the $[\text{CrTp}'_2]^+$ moiety both ligands are in the isomerized form, consistent with previous observations of regular octahedral

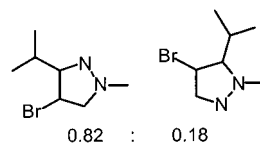


Figure 7. Orientations and occupancies of the disordered pyrazole ring in the Tp' anion in **5**.

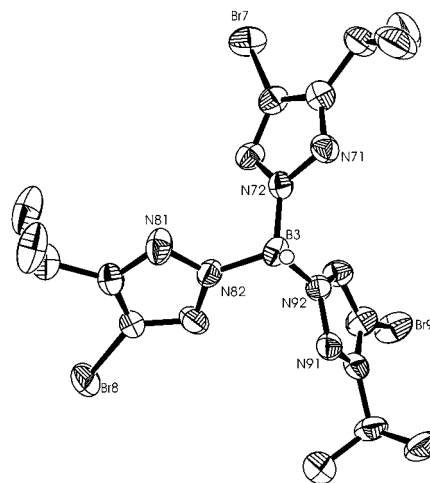


Figure 8. Molecular structure of Tp' anion in **5** showing only the major isomer of the two orientations of the disordered pyrazole ring. Thermal ellipsoids at 50% probability (hydrogen atoms are omitted for clarity).

complexes with this ligand.¹¹ The asymmetric unit contains two distinct Cr atoms, each of which lies on a crystallographic inversion center, and both of which have approximate octahedral symmetry. The Cr–N bond lengths vary between 2.008 and 2.065 Å in both half cations, and the N–Cr–N bond angles vary between 88.41° and 90.65°. The small deviations from strictly regular octahedral geometry are presumably due to the steric constraints of the bulky ligand. Both B centers display almost regular tetrahedral geometry with variation of N–B–N angles in the range 107.5°–109.9°. The Cr–N bond lengths are very similar to those reported for the unsubstituted Tp $\text{Cr}(\text{III})$ cations in the salts $[\text{CrTp}_2]^+[\text{CrCl}_4]^-$ and $[\text{CrTp}_2]^+[\text{CrCl}_3\text{Tp}]^-$.³¹

In all cases little material was obtained, so full characterization was not possible. However, IR spectroscopy revealed four peaks in the B–H region at 2529, 2460, 2364, and 2342 cm^{-1} . We have assigned the higher energy pair as the stretching modes of the octahedral cation and the lower energy pair as the two isomeric forms of the anion observed in the crystal structure. Indeed, the band at 2342 cm^{-1} is much less intense than band at 2364 cm^{-1} and the higher energy pair are of the same intensity. The mechanism of formation of this $\text{Cr}(\text{III})$ species is unclear and probably complex as indicated by the presence of both ligand isomers as the anion, but possibly involves disproportionation of the $\text{Cr}(\text{II})$ compound **3** and formation of a $\text{Cr}(0)$ byproduct which we have been unable to identify as yet. This disproportionation appears to be light induced: solutions in benzene could be heated at reflux in the dark for prolonged periods with no visible sign of decomposition; however, UV irradiation of the solution for 2 h caused reaction. IR analysis of the pentane-insoluble material gave a spectrum corresponding well with that of **5**. It would be difficult to reproduce exactly the constitution of **5** (as determined crystallographically) in terms of isomer distribution and solvent

(31) Li, C.-H.; Chen, J.-D.; Liou, L.-S.; Wang, J.-C. *Inorg. Chim. Acta* **1998**, 269, 302–309.

Table 5. Selected Bond Lengths and Angles in **5**

Cr1–N11	2.037(4)	N11–Cr1–N21	89.85(15)
Cr1–N21	2.008(4)	N11–Cr1–N31	88.69(14)
Cr1–N31	2.062(3)	N21–Cr1–N31	90.65(14)
Cr2–N41	2.065(4)	N41–Cr2–N51	90.62(15)
Cr2–N51	2.022(4)	N41–Cr2–N61	88.41(14)
Cr2–N61	2.051(4)	N51–Cr2–N61	89.64(15)
N12–B1	1.547(6)	N12–B1–N22	108.5(3)
N22–B1	1.533(6)	N12–B1–N32	108.1(4)
N32–B1	1.544(6)	N22–B1–N32	108.0(4)
N42–B2	1.543(7)	N42–B2–N52	107.5(4)
N52–B2	1.541(7)	N42–B2–N62	109.9(4)
N62–B2	1.509(7)	N52–B2–N62	108.2(4)
N72–B3	1.526(7)	N72–B3–N82	108.9(4)
N82–B3	1.560(7)		

incorporation into the crystal lattice; however, it seems clear that in benzene solution **3** is prone to photoinduced oxidation and rearrangement with the exact nature of the products being sensitive to the conditions employed. It is interesting to note that **4** was not observed as a product in any of these reactions.

Various techniques have been reported as reliable indicators of the hapticity of Tp ligands both in the solid state and in solution. Unambiguous structural assignment in the solid state is provided by X-ray crystallography, while ^{11}B NMR chemical shifts have been used to assign coordination geometry of Tp complexes in solution.³² The B–H stretch in the IR spectrum of a variety of $\text{MTp}^{i-\text{Pr}}\text{L}_n$ complexes has been correlated with the hapticity of the $\text{Tp}^{i-\text{Pr}}$ ligand ($\kappa^2 \sim 2470\text{ cm}^{-1}$ and $\kappa^3 > 2530\text{ cm}^{-1}$).^{25,33} As a point of comparison between the $\text{Tp}^{i-\text{Pr}2}$ and Tp' ligands, the B–H stretch of **1** is 2504 cm^{-1} as opposed to 2550 cm^{-1} for $\text{FeTp}^{i-\text{Pr}2}\text{Cl}$.²¹

Table 6 details the $\nu_{\text{B-H}}$ bands for all the crystallographically characterized complexes containing the Tp' ligand (with reported IR data). Analysis is slightly complicated by the presence of two Tp' ligands in most of the molecules and hence multiple stretching modes (Akita's analysis is based primarily on mono Tp compounds). However, it seems clear that, for κ^3 compounds (taking only the higher energy mode into account for 6-coordinate compounds), $\nu_{\text{B-H}}$ lies in the range $2496\text{--}2525\text{ cm}^{-1}$ with only $\text{CoTp}'(\text{NCS})$ lying outside this region, and is lower in energy than that for $\text{Tp}^{i-\text{Pr}2}$. Comparison of the data with reported $\nu_{\text{B-H}}$ for compounds containing the $\text{Tp}^{i-\text{Pr}}$ ligand reveals that, despite the electron-withdrawing Br group, $\nu_{\text{B-H}}$ is higher in energy in Tp' compounds.¹¹ It has been noted that the electron-donating ability of Tp^{R} can be assessed on the basis of $\nu_{\text{B-H}}$ in NaTp^{R} and KTp^{R} , where the anomaly of a Br substituent in the 4-position causing a higher energy shift is also apparent.²⁵ The $\text{Tp}^{\text{Me}2}$ analogue of $[\text{Rh}(\text{H})_2(\text{PMe}_3)_4]^+[\text{Tp}]^-$

Table 6. Values of $\nu(\text{B-H})$ for Complexes Containing the Tp' Ligand

compound	$\nu(\text{B-H})$ (cm^{-1})	ref
1	2504 ^a	this work
2	2506 ^a	this work
3 ^b	2496, 2368 ^a	this work
4 ^b	2524, 2489 ^a	this work
5 ^b	2529, 2460, 2364, 2342 ^a	this work
KTp'^{c}	2120–2320 ^d	11
TITp'^{c}	2448 ^d	11
TITp'^{c}	2438 ^a	this work
$\text{CoTp}'\text{Cl}$	2520 ^c	11
$\text{CoTp}'(\text{NCS})$	2550 ^d	11
$\text{Co}(\text{Tp}')_2^{\text{b}}$	2520, 2500, 2480 ^d	11
$\text{MoTp}'(\text{NO})(\text{CO})_2^{\text{c}}$	2500 ^d	11
$[\text{CoTp}'(\text{NCS})_2]_2$	2510 ^a	34

^a Obtained as KBr disks. ^b Contains rearranged ligand. ^c Entries in italics are not crystallographically characterized. ^d Obtained as Nujol mulls.

has $\nu_{\text{B-H}}$ of 2431 cm^{-1} , which is of higher frequency than that observed for **5**. A lack of examples for further comparison prevents a correlation of $\nu_{\text{B-H}}$ with binding mode for Tp' ; however, Carmona reports that a distinction between κ^0 and κ^1 modes on the basis of ^{11}B NMR shifts and IR data is not possible for $\text{Tp}^{\text{Me}2}$ in the context of their compounds.

Conclusion

We have synthesized and structurally characterized stable, high-spin, 4-coordinate TpMCl compounds (where $\text{M} = \text{Fe}$ and Mn) with the sterically intermediate ligand Tp' . In the formation of these compounds Tp' behaves analogously to ligands with bulkier substituents in the 3-position.²⁰ Attempted isolation of a 4-coordinate Cr compound was unsuccessful; however, we were able to isolate and structurally characterize both 5- and 6-coordinate isomers of CrTp'_2 . Presumably the larger size of Cr with respect to Mn is sufficient to make the TpCrCl unstable with respect to coordination of a second Tp' ligand. The 5-coordinate isomer **3** is labile in solution, in pentane it is converted via a borotropic rearrangement to the 6-coordinate isomer **4**, and in benzene solution it is photosensitive and decomposes to give, as one of the products, $[\text{CrTp}'_2]^+[\text{Tp}]^-$ which contains a rare example of a Tp ligand acting as a noncoordinating counterion.

Acknowledgment. We thank Dr. S. Barlow for many valuable discussions and for assistance in acquiring magnetic data, Dr. P. Halasyamani for collecting X-ray crystallography data, and the EPSRC for a studentship (T.J.B.).

Supporting Information Available: Complete tables of refined position coordinates, anisotropic thermal parameters, and complete tables of bond lengths and angles for **1–5**. This material is available free of charge via the Internet at <http://pubs.acs.org>.

IC010125K

(32) Northcutt, T. O.; Lachicotte, R. J.; Jones, W. D. *Organometallics* **1998**, *17*, 5148–5152.

(33) Akita, M.; Hashimoto, M.; Hikichi, S.; Moro-oka, Y. *Organometallics* **2000**, *19*, 3744–3747.

(34) Trofimenko, S.; Calbrese, J. C.; Kochi, J. K.; Wolowicz, S.; Hulsbergen, F. B.; Reedijk, J. *Inorg. Chem.* **1992**, *31*, 3943–3950.